Free Radical Biology and Medicine 234 (2025) 192–202

Contents lists available at ScienceDirect

Free Radical Biology and Medicine

journal homepage: www.elsevier.com/locate/freeradbiomed

3-Bromopyruvate boosts the effect of chemotherapy in acute myeloid leukemia by a pro-oxidant mechanism

Joana Pereira-Vieira [a,b,*], Sara Granja [a,b,c,d], Sónia Pires Celeiro [a,b], Catarina Barbosa-Matos [a,b], Ana Preto [e,f], Odília Queirós [g], Young Hee Ko [h], Margarida Casal [e,f], Fátima Baltazar [a,b,**]

[a] Life and Health Sciences Research Institute (ICVS), School of Medicine, University of Minho, Campus of Gualtar, 4710-057, Braga, Portugal
[b] ICVS/3B's - PT Government Associate Laboratory, Braga, Guimarães, Portugal
[c] REQUIMTE/LAQV, Escola Superior de Saúde, Instituto Politécnico do Porto, Rua Dr. António Bernardino de Almeida, 4200-072, Porto, Portugal
[d] Department of Pathological, Cytological and Thanatological Anatomy, ESS|P.PORTO, 4200-072, Porto, Portugal
[e] CBMA—Centre of Molecular and Environmental Biology, Department of Biology, University of Minho, 4710-057, Braga, Portugal
[f] IBS—Institute of Science and Innovation for Bio-Sustainability, University of Minho, 4710-057, Braga, Portugal
[g] UNIPRO—Oral Pathology and Rehabilitation Research Unit, University Institute of Health Sciences, CESPU, CRL, 4585-116, Gandra, Portugal
[h] KoDiscovery, LLC, Institute of Marine and Environmental Technology (IMET) Center, 701 East Pratt Street, Baltimore, MD, 21202, USA

ARTICLE INFO

Keywords:
Blood cancer
Cancer metabolism
Cytarabine
Daunorubicin
Oxidative stress

ABSTRACT

Acute myeloid leukemia (AML) comprises a diverse group of blood cancers with varying genetic, phenotypic, and clinical traits, making development of targeted therapy challenging. Metabolic reprogramming in AML has been described as relevant for chemotherapy effectiveness. 3-Bromopyruvate (3-BP) is an anticancer agent that undermines energy metabolism of cancer cells. However, the effect of 3-BP in hematologic malignancies, such as AML, needs further investigation. Thus, we aimed to explore 3-BP as a chemo-sensitizing agent in AML. Different approaches of combining 3-BP with classical chemotherapy (daunorubicin and cytarabin) were tested in diverse AML cell lines. Cell sensitivity to the different drug combinations was analyzed by Trypan blue staining. The effect of pre-treatment with a non-toxic concentration of 3-BP was assessed on the AML cell metabolic profile (Western blot and immunofluorescence), mitochondrial activity (cytometry flow), and antioxidant capacity (colorimetric detection kit). KG-1 and MOLM13 cells showed increased sensitivity to chemotherapy (decreased EC_{50} values) after exposure to a non-toxic concentration (5 μM) of 3-BP. In both cell lines, 5 μM 3-BP decreased glucose consumption without changing extracellular lactate levels. 5 μM 3-BP treatment increased reactive oxygen species levels and decreased cell antioxidant capacity by depleting reduced glutathione levels in both KG-1 and MOLM13 cells. Our results demonstrate that non-toxic concentrations of 3-BP enhance the effect of classical chemotherapy in AML cells through a pro-oxidant mechanism. These data unveiled a new approach for AML treatment, using 3-BP or other pro-oxidant agents as co-adjuvants of chemotherapy, subsiding chemotherapy-induced side effects.

1. Introduction

Acute Myeloid Leukemia (AML) is the most common acute leukemia in adults and is characterized by clonal expansion of immature myeloblasts [1]. It is a heterogeneous disease with rapid development, where a fast therapeutic intervention is necessary [2]. Currently, standard treatment includes the combination of cytarabine (Ara-C) with an anthracycline, such as daunorubicin (DNR) or idarubicin. The treatment protocol consists of continuous administration of cytarabine for 7 days and of an anthracycline on each of the first 3 days, known as the "7 + 3"

* Corresponding author. Life and Health Sciences Research Institute (ICVS), School of Medicine, University of Minho, Campus of Gualtar, 4710-057, Braga, Portugal.
** Corresponding author. Life and Health Sciences Research Institute (ICVS), School of Medicine, University of Minho, Campus of Gualtar, 4710-057, Braga, Portugal.
E-mail addresses: joanavieira@med.uminho.pt (J. Pereira-Vieira), gcs@ess.ipp.pt (S. Granja), id9536@alunos.uminho.pt (S.P. Celeiro), catarina.barbosamatos@research.fchampalimaud.org (C. Barbosa-Matos), apreto@bio.uminho.pt (A. Preto), odilia.queiros@iucs.cespu.pt (O. Queirós), youngheeko@kodiscovery.org (Y.H. Ko), mcasal@bio.uminho.pt (M. Casal), fbaltazar@med.uminho.pt (F. Baltazar).

https://doi.org/10.1016/j.freeradbiomed.2025.04.017
Received 10 February 2025; Received in revised form 9 April 2025; Accepted 10 April 2025
Available online 11 April 2025

cycle regimen [3]. To improve the chances of remission, patients with specific mutations can be treated with targeted drugs in combination with cytotoxic induction therapy. AML patients with mutated fms-like tyrosine kinase 3 (*FLT3*) may be considered to receive intensive chemotherapy in combination with the FLT3 inhibitor midostaurin [4], while patients with isocitrate dehydrogenase (*IDH)1 or IDH2* mutations may be treated with ivosidenib or enasidenib [5], respectively. More recently, the inhibitor of the antiapoptotic BCL-2 protein (venetoclax) became available for AML patients above 75 years, or with other medical conditions that preclude the use of intensive chemotherapy [6]. Despite response to chemo- and targeted therapy, disease-free survival is low, with one in every four AML patients relapsing five years after first diagnosis with chemotherapy-associated resistance [7]. Thus, new and effective therapeutic approaches are urgent to improve the outcome of the disease.

A common feature of cancer cells is metabolic reprogramming, which is mainly associated with the acquisition of an "aerobic" glycolytic phenotype (Warburg effect) [8,9]. Even though this is a less energetically efficient process, cancer cells take advantage of this metabolic switch, for example by diverging biosynthetic precursors to anabolic reactions and developing antioxidant defenses [10]. AML blast metabolism is primarily dependent on mitochondrial oxidative phosphorylation (OXPHOS) for growth and survival [11,12]. To sustain their high proliferation rates and metabolic demand, leukemic blasts use different metabolic strategies, including glycolytic metabolism [13–17], as our group reported recently that resistance to Ara-C involves metabolic adaptations with different sensitivities to metabolic inhibitors [18].

Highly glycolytic cancer cells protect themselves from intracellular acidification by exporting the excess of the glycolytic end-products, such as lactate and protons, via the Monocarboxylate Transporters (MCTs) [19]. MCTs play a key role in tumor metabolism, being the isoforms MCT1 and MCT4 commonly overexpressed in cancer cells, representing promising targets for therapy [20]. Recently, Saulle et al. (2021) demonstrated that inhibition of MCT1 or MCT4 impairs leukemic cell proliferation [19]. Additionally, Lopes-Coelho et al. (2017) suggested that the AML cells' preferential localization near the bones, to take advantage of the growth factor gradient, stimulates cell proliferation and upregulates the expression of MCT1 [21]. MCTs can also be explored in cancer therapy through their role as mediators of the transport of antitumor molecules which function as MCT substrates [22].

3-bromopyruvate (3-BP) is a small alkylating molecule derivative of pyruvate and analog of lactate, with anti-tumor effects in different *in vitro* and *in vivo* cancer models [16–21], which is described to permeate cells through MCT1 [22]. 3-BP has two major anti-cancer mechanisms: it blocks energetic metabolism and induces cell death [23,24]. Although the potential effect of 3-BP has been explored in different solid tumor models [16], little is known about the effect of 3-BP, especially as a chemo-sensitizing agent, in AML. Thus, we propose to explore this therapeutic strategy, by combining 3-BP with chemotherapeutic agents, and identify the mechanisms involved.

2. Materials and methods

2.1. Cell lines and culture conditions

AML cell lines were obtained from DSMZ-German Collection of Microorganisms and Cell Cultures GmbH: one monocytic (MOLM-13), two promyelocytic (HL-60, NB-4) and one myelocytic (KG-1) cell lines. Cells were maintained and routinely subcultured in culture flasks at a cell density between 1×10^5 and 1×10^6 cells/mL. Cells were grown in a complete medium consisting of RPMI (Sigma-Aldrich, St. Louis, MO, USA) supplemented with 10 % Fetal Bovine Serum (FBS, Sigma-Aldrich) and 1 % penicillin/streptomycin (PenStrep, PanBiotech, Aidenbach, Germany). Cell cultures were maintained in a humidified incubator at 37 °C and a 5 % CO_2 atmosphere. To obtain enough biomass to perform the assays, cells were grown to high densities, but not exceeding 1×10^6 viable cells/mL and with cell viability up to 90 %. Viable cell estimation was performed by adding 1:1 cell suspension to 0.2 % trypan blue (sc-216028, Santa Cruz Biotechnology, Dallas, TX, USA), and cells were counted in a Neubauer chamber.

2.2. Drugs and stock solution preparation

3-Bromopyruvate (3-BP, Sigma-Aldrich) stock solutions (2–20 mM) were prepared by dissolving 3-BP into cold PBS, and then filter-sterilized (0.22 μm filters). Working solutions were prepared by appropriate dilutions in a complete RPMI medium. The amount of 3-BP solution in PBS was constant and corresponded to 10 % of the total medium volume. Stock solutions of cytarabine (Ara-C, C3350000, Sigma-Aldrich, Strasbourg, France) and daunorubicin (DNR, D0125000, Sigma-Aldrich) were prepared in DMSO (Sigma-Aldrich), 10 mM and 50 mM, respectively. N-Acetyl-L-cysteine (NAC, Sigma-Aldrich) stock solution (60 mM) was prepared in PBS. DNR, Ara-C, and NAC stock solutions were stored at −20 °C until use. 3-BP, DNR, Ara-C, and NAC working solutions were freshly prepared in a complete RPMI medium.

2.3. Cell viability determination

1×10^5 cells/well were seeded in 24-well plates and exposed to a range of increasing Ara-C concentrations (0.05–10 μM), DNR (0.001–0.5 μM) and 3-BP (1–50 μM) for 16, 24 and 48 h. Drug vehicles, 0.1 % DMSO, and PBS were used as controls. Cells were counted using the Trypan blue assay, and cell viability and EC_{50} values for Ara-C, DNR, and 3-BP were determined and normalized for the control.

2.4. Western blotting

Protein expression analysis was performed in cell lysates as previously described [18]. Briefly, cell lysates were prepared from cultured cells using a lysis buffer (1 % (v/v) Triton X-100 and 1 % (v/v) NP-40 (Sigma-Aldrich) in ultrapure water; 1:7 protease inhibitor cocktail (Roche®, Basel, Switzerland) and 1:100 phosphatase inhibitor (Sigma-Aldrich). After washing with PBS, cells were lysed in 100 μL of lysis buffer for 15 min at 4 °C. Then, lysates were homogenized (vortex), centrifuged at high speed, and supernatants were collected. Protein concentration was determined using the Bradford assay (B6916, Sigma-Aldrich). Samples were then separated by 10 % SDS/PAGE. Proteins were transferred to nitrocellulose membranes (Amersham Biosciences®, Amersham, United Kingdom) at 100 V for 90 min. For immunostaining, membranes were blocked with 5 % (w/v) BSA in TBS containing 0.1 % (v/v) Tween-20 (TBS-T). Membranes were incubated overnight at 4 °C with glucose transporter (GLUT) 1 (1:500, ab15309), hexokinase (HK) II (1:2000, ab104836), MCT1 (1:500, sc-365501); MCT4 (1:500, sc-376465), lactate dehydrogenase (LDH) A (1:2000, sc-137243), IDH1 (1:500, sc-515396), IDH2 (1:500, sc-374476), β-actin (1:1000, sc-1616) and β-tubulin (1:20,000, ab6046) primary antibodies, followed by two washing steps (15 min each) in TBS-T and incubation with horseradish peroxidase-conjugated secondary antibodies for 1 h at room temperature (RT) (1:5000, sc-516102 and sc-2357). The signal was detected in Sapphire Biomolecular Imager (Azure Biosystems, Dublin, CA, USA) using the Westen Bright Sirius HRP Substrate Kit (K-12043-D10, Advansta, San Jose, CA, USA). Each immunoblot was performed at least three times, and the ones selected for figures are from representative experiments.

2.5. Extracellular lactate and glucose quantification

Cells were plated in 24-well plates at a density of 5×10^5 cells/well and treated with 5 μM of 3-BP. Cell culture supernatants were collected at 0 and 24 h, and extracellular lactate and glucose were quantified as previously described [25], using the Lactate and Glucose-LQ Colorimetric Assays (Spinreact, Girona, Spain), according to the

manufacturer's instructions. The obtained values were normalized for the total number of cells (determined by Trypan blue). Glucose consumption was determined by the difference between glucose levels at time points 0 and 24 h. Data are expressed as μg/10^6 cells.

2.6. Immunofluorescence

5×10^5 cells were centrifuged onto a slide by cytocentrifugation and fixed for 20 min with cold methanol at −20 °C. Slides were washed twice with 1x PBS and blocked with 5 % BSA (Sigma-Aldrich) in 1x PBS - 0.1 % Tween 20 (PBS-T) for 1h at RT. After blocking, cells were incubated overnight with GLUT1, MCT1, and MCT4 primary antibodies. After washing (twice), slides were incubated with goat anti-mouse conjugated to AlexaFluor 488 (1:500, A11001, Invitrogen) and goat anti-rabbit conjugated to AlexaFluor 568 (1:500, A11036, Invitrogen) secondary antibodies for 1h at RT. Slides were mounted on Fluorshield with DAPI (F6057, Sigma-Aldrich), protected from light, and images were captured by a fluorescence microscope (BX61; Olympus®, Tokyo, Japan).

2.7. Annexin/propidium iodide assay

KG-1 and MOLM13 cells (5×10^5 cells/well) were plated on 6-well plates and pre-treated with 5 μM of 3-BP for 16 h. Cells were collected and washed with PBS. After centrifugation (900 rpm, 5 min), the supernatant was discarded, and the pellet resuspended in 1 mL of Binding Buffer. 8 μL of FITC annexin V (556419, BD Pharmingen) and 30 μL of propidium iodide (PI, 50 μg/mL, P1304MP, Invitrogen), were added to 300 μL of Binding Buffer. Then, samples were incubated for 15 min at RT, protected from light. Data were acquired on an LSRII flow cytometer (BDBiosciences®) and FACS Diva was used as the acquisition software. The percentage of cells in each phase was analyzed using the FlowJo 7.6 (Tree Star®) software.

2.8. Reactive oxygen species levels and mitochondrial function evaluation

KG-1 and MOLM13 cells were plated in 6-well plates at a density of 5×10^5 cells/well and pre-treated with 5 μM of 3-BP. Then, cells were incubated with the molecular probes for 2h at 37 °C and 5 % CO_2. For measurement of reactive oxygen species (ROS) production, cells were incubated with 400 nM of Dihydroethidium (DHE, Molecular Probes). For mitochondrial activity, cells were incubated with 50 nM Mitotracker Red (MR) and 30 nM Mitotracker Green (MG) both from Molecular Probes®, Eugene, OR, USA. Cells were then washed with 1x PBS, and Data were acquired on an LSRII flow cytometer (BDBiosciences®) and FACS Diva was used as the acquisition software. At least 50,000 events were acquired, and the data was analyzed using the FlowJo 7.6 (Tree Star®) software. MR and MG were used to measure mitochondrial polarization and mitochondrial mass, respectively. Mitochondrial activity was given by the mitochondrial polarization/mitochondrial mass ratio.

2.9. Glutathione quantification

KG-1 and MOLM13 cells were pre-treated with 3-BP in T75 flasks. Then cells were collected, and part of the volume was used for cell counting. The remaining (at least 1×10^6 cells) were pelleted by centrifugation and resuspended in a 5 % sulfosalicylic acid solution, for deproteinization. The glutathione colorimetric detection kit was used to measure total glutathione and oxidized glutathione (GSSG) content, according to the manufacturer's instructions (Invitrogen™, Thermo Fisher Scientific, Waltham, MA, USA). A 2-vinylpyridine solution was used to block free GSH present in the samples, to determine GSSG content. A spectrophotometer (Varioskan® Flash; ThermoFisher Scientific, Waltham, MA, USA) was used to measure the absorbance at 405 nm. Data was normalized to the number of cells (μM/10^6 cells).

2.10. Statistical analysis

Statistical analysis was performed using the GraphPad Prism 10.3.0 software. Data are presented as the mean ± standard deviation (SD) from 2 or 3 independent experiments. Differences between groups were considered statistically significant at $p < 0.05$, and a trend was considered at $0.05 < p \leq 0.10$.

3. Results

3.1. Acute myeloid Leukemia cells present different metabolic profiles

The different AML cell lines presented diverse patterns of lactate production (Fig. 1A–C). The promyelocytic cells (NB-4, and HL-60) displayed significantly higher levels of extracellular lactate than KG-1 and MOLM13 cells at 24 h (Fig. 1A). Regarding glucose consumption, no significant differences were observed between the cell lines (Fig. 1B). When comparing the ratio of lactate production/glucose consumption, MOLM13 cells presented the lowest glycolytic profile compared to NB-4, HL-60, and KG-1 cell lines (Fig. 1C).

The expression of different proteins involved in glucose metabolism, namely GLUT1, HKII, LDHA, MCT1, and MCT4, as well as IDH1 and IDH2, cytoplasmatic and mitochondrial tricarboxylic acid (TCA) cycle enzymes, were analyzed in basal conditions for all AML cell lines by Western blot (Fig. 2 and Fig. S1). MOLM13 cells exhibited lower levels of glucose and lactate transporters (GLUT1, MCT1, and MCT4) and the enzyme LDHA (responsible for converting pyruvate into lactate), compared to the other cell lines, particularly NB-4 cells (Fig. 2A and B). These findings are consistent with the previous results. Additionally, the location of membrane transporters was evaluated by immunofluorescence, confirming their presence at the cell membrane (Fig. 2C and Fig. S2). No differences were observed regarding HKII and IDH1 expression among the cell lines (Fig. 2A and B), but MOLM13 cells displayed higher levels of IDH2 expression compared to other cell lines (Fig. 2A and B). Thus, AML cell lines showed different metabolic profiles: HL-60 and NB-4 cells were the most glycolytic, followed by KG-1 and MOLM13 cells.

3.2. 3-Bromopyruvate treatment sensitizes MOLM13 and KG-1 cells to chemotherapy

Next, we evaluated the response of AML cells to 3-BP, a glycolytic inhibitor. Cell viability was estimated after 24 h and 48 h of drug treatment and cell viability decreased in a dose (but not time) dependent manner for all AML cell lines (Figs. S3A–D). MOLM13 cells were the most sensitive to 3-BP compared to HL-60, NB-4, and KG-1 cells at 24 h and 48 h (Figs. S3E and F). Considering previous studies that demonstrated an enhancement of the chemotherapy effect when combined with a metabolic inhibitor [25–28], we proposed to test two different approaches (Fig. 3A and Fig. S4A). First, we evaluated the effect of combining 3-BP with DNR or Ara-C simultaneously in AML cell lines (Fig. S4A) for 48 h (Figs. S4B–I and Table 1). In these assays, we used the 3-BP concentration based on estimated $EC_{12.5}$ and EC_{25} values with the drugs and evaluated cell viability. A slight cell viability decrease was observed in KG-1 for Ara-C and in MOLM13 for Ara-C and DNR, where both EC_{50} values decreased at least twice for the combination with 3-BP EC_{25} plus drugs (Table 1 and Figs. S4D and I). We also observed that both combinations with 3-BP plus Ara-C decreased about 5-fold the EC_{50} value for Ara-C in MOLM13 cells (Table 1 and Fig. S4H). No difference was observed in HL-60 and NB-4 (Fig. S4B-C and F-G, and Table 1).

As a second approach, to further decrease the toxicity of the drug combination, we evaluated the effect of a pre-treatment with a non-toxic concentration of 3-BP for 16 h, followed by the chemotherapeutic drugs (Fig. 3A). Different 3-BP concentrations were tested in all AML cell lines for a 16 h period, and 5 μM 3-BP was the one selected where no cell viability decrease was observed (Fig. 3B). Then, after the pre-treatment

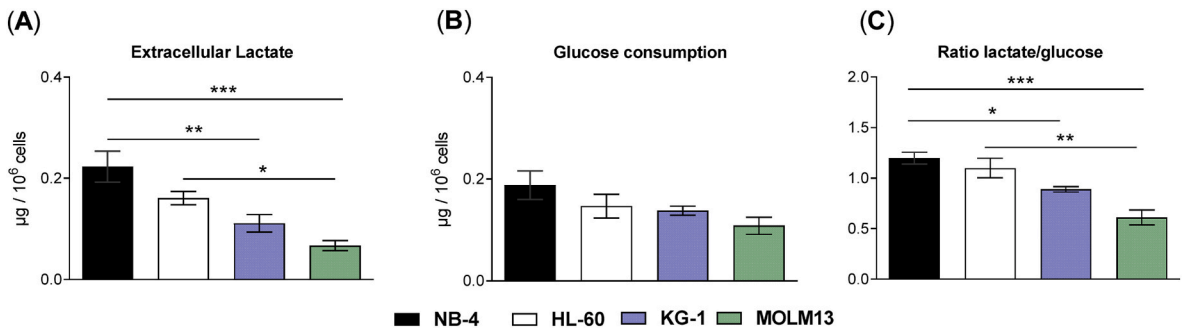

Fig. 1. Glycolytic profile in AML cell lines in basal conditions. (A) Levels of extracellular lactate, (B) glucose consumption, and (C) ratio of lactate/glucose were evaluated after 24 h for NB-4, HL-60, KG-1, and MOLM13 cells. Results are presented as mean ± SD of three independent experiments. Statistical significance was calculated by one-way ANOVA followed by Tukey's Multiple Comparison Test: *p ≤ 0.05; **p ≤ 0.01; ***p ≤ 0.001.

with 5 μM 3-BP, cell viability, and EC_{50} values were determined for Ara-C and DNR in all AML cell lines (Table 2 and Figs. S5A–H). Pre-treatment with 3-BP only sensitized KG-1 and MOLM13 cells to chemotherapy, decreasing cell viability, and no effect was observed in HL-60 and NB-4 cells (Fig. S5C–D and G–H). The EC_{50} values of DNR and Ara-C decreased about 4-fold in KG-1 cells and the EC_{50} values of Ara-C, but not in DNR, decreased 5-fold in MOLM13 cells (Table 2).

In general, both strategies enhance the effect of both drugs in KG-1 and MOLM13 cells compared to HL-60 and NB-4 cells, with a greater effect observed with the 3-BP pre-treatment approach. Subsequently, we selected the KG-1 and MOLM13 cell lines to investigate the mechanism by which pre-treatment with 5 μM of 3-BP increases cell sensitivity to chemotherapy.

3.3. 5 μM 3-Bromopyruvate does not significantly alter glycolytic metabolism of AML cells

The blockage of energetic metabolism is the major anti-cancer mechanism described for 3-BP [16,17]. Thus, even though 5 μM 3-BP did not affect cell viability, we evaluated the effect of this concentration on the glycolytic profile of AML cells. The extracellular lactate levels were not altered in any of the cell lines by the pre-treatment conditions, but an increase in the ratio of lactate production/glucose consumption was observed for KG-1 and MOLM13 cells, as well as a slight decrease in glucose consumption only for MOLM13 cells (Fig. 4A–C,E-G). Next, the mitochondrial activity was also determined by evaluating the ratio of Mitotracker Red/Mitotracker Green by flow cytometry, where we observed a trend to decrease of mitochondrial activity for KG-1 cells pre-treated with 3-BP (Fig. 4D), and no difference was observed for MOLM13 cells (Fig. 4H). Thus, the non-toxic concentration of 3-BP does not significantly interfere with the glycolytic profile and mitochondrial activity of AML cells (Fig. 4).

Additionally, as low concentrations of 3-BP (5 μM) can activate cell death pathways [24,29], cell death was evaluated in KG-1 and MOLM13 cells were treated with 5 μM 3-BP (Fig. S6). The flow cytometry results showed that this concentration of 3-BP did not induce apoptosis or necrosis in any of the cell lines, in accordance with the previous cell viability results.

3.4. 5 μM 3-Bromopyruvate decreases the antioxidant capacity of AML cells

The levels of ROS and glutathione were assessed in KG-1 and MOLM13 cell lines to evaluate their antioxidant capacity upon exposure to 5 μM 3-BP (Fig. 5). For KG-1, we observed a significant increase in total glutathione (GSH), oxidized (GSSG), and reduced GSH (Fig. 5A–C) with a significant decrease in the ratio of reduced GSH (active) and GSSG (inactive, Fig. 5D). In addition, treatment with 5 μM 3-BP induced a significant increase in ROS production by KG-1 cells, which was reversed by NAC, an antioxidant, (Fig. 5E). These results suggest that, despite the increase in different forms of GSH, 3-BP decreases the antioxidant capacity of KG-1 cells by an increase in the production of ROS. For MOLM13, there was no difference in total GSH levels upon treatment with 3-BP, but there was a significant increase in GSSG and a decrease in reduced GSH (Fig. 5E–H) with a significant decrease in the ratio of reduced GSH and GSSG (Fig. 5I). For ROS production, there was a tendency for MOLM13 cells treated with 5 μM 3-BP to increase the levels of ROS compared to PBS, while NAC alone was able to significantly decrease the levels of ROS compared to PBS and 5 μM 3-BP. Still, 3-BP plus NAC was able to further decrease the levels of ROS when compared to NAC (Fig. 5J).

Assuming that ROS production could be a mechanism by which 3-BP pre-treatment enhanced the effect of chemotherapy, we evaluated the effect of NAC, a GSH precursor capable of neutralizing ROS, on the drug effect in both KG-1 and MOLM13 cells pre-treated with 5 μM 3-BP (Fig. 6). For KG-1 cells, 20 μM NAC reverted the effect of pre-treatment with 5 μM 3-BP in both drugs, increasing the EC_{50} values for DNR in KG-1 cells pre-treated with NAC and NAC plus 3-BP (Fig. 6A), while the EC_{50} values of Ara-C were similar with untreated KG-1 cells (Fig. 6B). For MOLM13, NAC decreased the cell sensitivity to DNR, increasing their EC_{50} values in MOLM13 treated with NAC and NAC plus 3-BP (Fig. 6C). For Ara-C, NAC alone was able to decrease the cell viability when compared to MOLM13 cells treated with PBS (Fig. 6D). Thus, using the NAC, a scavenger of ROS, to treat cells can not only protect them from the effect of 3-BP and chemotherapy but may also enhance their effect, depending on the cell line type and drug.

4. Discussion

AML is a neoplastic disease characterized by genetic diversity, affecting the differentiation and proliferation of cells, with an accumulation of immature cells, the myeloid blasts. This cell heterogeneity has compromised the understanding of AML development and progression but also the classification and the effectiveness of the therapeutic approaches [1–4]. The heterogeneous nature of AML has also hampered the identification of a key metabolic signature, contributing to the controversy found in the literature [11–15,29–32]. In the present study, we started to characterize metabolically four human AML cell line models: MOLM13, an M5a-derived cell line that carries internal tandem duplication of FLT3; KG-1 cell line derived from a patient with erythroleukemia; NB-4 cell line from a patient with acute promyelocytic leukemia; HL-60 cell line from a patient with acute myeloid leukemia that can be also used for induction of differentiation studies [33]. The metabolic profiles observed in our study align with previous findings that classify NB-4 and HL-60 cells as more glycolytic, mainly due to AKT/mTORC1 activation [31], while MOLM13 cells favor OXPHOS [18,34]. This difference may be explained by variations in mitochondrial activity and glycolytic profile, which influence their sensitivity to drugs

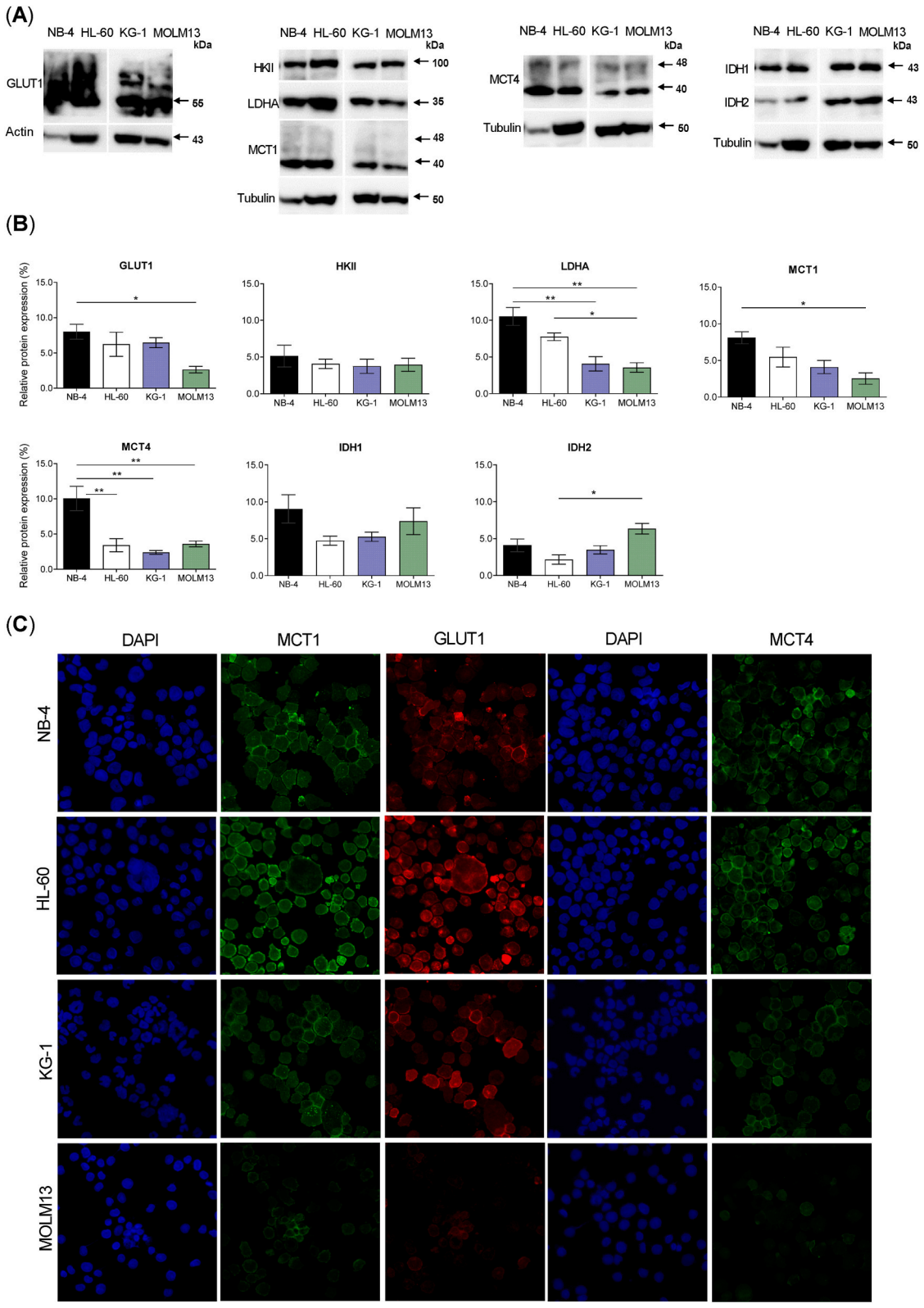

Fig. 2. Characterization of metabolism-associated protein expression and subcellular localization in AML cell lines. (A) Representative blots of two independent experiments and (B) analysis of the relative expression of GLUT1, HKII, LDHA, MCT1, IDH1, IDH2, and MCT4 proteins assessed by Western blot in the NB-4, HL-60, KG-1, and MOLM13 cell lines at 24 h, using tubulin or actin as loading controls. Results were quantified using the ImageJ software and normalized to respective loading control. Results are presented as mean ± SD. Statistical significance was estimated by one-way ANOVA followed by Tukey's Multiple Comparison Test: *$p \leq 0.05$; **$p \leq 0.01$. (C) Localization of MCT1, MCT4 (green), and GLUT1 (red) is shown at the cell membrane of HL-60, NB-4, MOLM13, and KG-1 cells by immunofluorescence. Cell nuclei were counterstained with DAPI (blue). Images are representative of two independent experiments that were taken using the microscope Olympus BX61 at 200x (scale bar 50 μm). (For interpretation of the references to color in this figure legend, the reader is referred to the Web version of this article.)

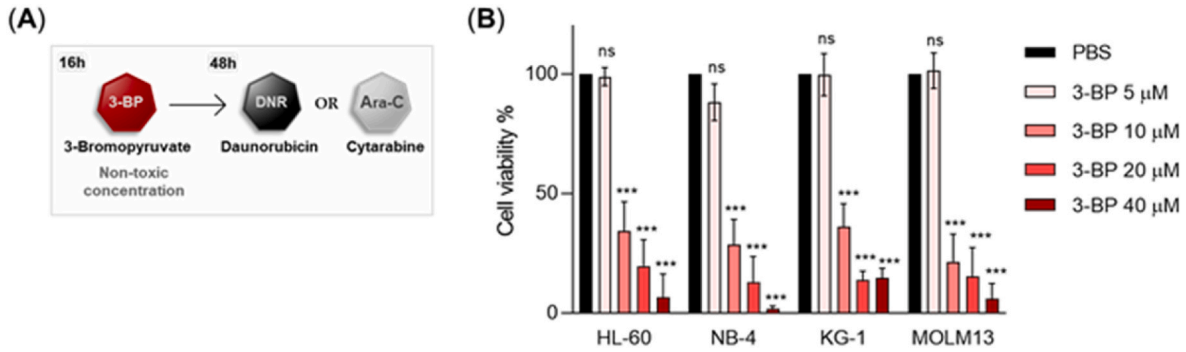

Fig. 3. Determination of a non-toxic concentration of 3-bromopyruvate (3-BP) in AML cell lines. (A) Scheme of AML pre-treatment with 3-BP (16 h) followed by treatment with daunorubicin (DNR) or cytarabine (Ara-C) for 48 h. (B) Determination of a non-toxic concentration of 3-BP after 16 h for AML cell lines using the Trypan blue assay. Values are presented as cell viability relative to vehicle-treated cells normalized to 100 %. Values are given as mean ± SD and results are from at least three independent experiments with at least two replicates each. Statistical significance was calculated by one-way ANOVA followed by Tukey's Multiple Comparison Test: ***$p \leq 0.001$; ns, not significant. (For interpretation of the references to color in this figure legend, the reader is referred to the Web version of this article.)

Table 1
Effect of combination with 3-bromopyruvate (3-BP) and chemotherapy in AML cell lines.

	EC_{50} values ± SD (μM) for DNR and Ara-C with and without 3-BP							
Treatment	HL-60	Fold change[a] (EC_{50})	NB-4	Fold change[a] (EC_{50})	KG-1	Fold change[a] (EC_{50})	MOLM13	Fold change[a] (EC_{50})
DNR	0.029 ± 0.021	–	0.034 ± 0.022	–	0.052 ± 0.027	–	0.018 ± 0.008	–
DNR + 3-BP $EC_{12.5}$	0.033 ± 0.021	0.9 ^{ns}	0.033 ± 0.017	1.0 ^{ns}	0.062 ± 0.006	0.8 ^{ns}	0.017 ± 0.008	1.1 ^{ns}
DNR + 3-BP EC_{25}	0.037 ± 0.026	0.8 ^{ns}	0.034 ± 0.026	1.0 ^{ns}	0.049 ± 0.019	1.1 ^{ns}	0.009 ± 0.003	2.0^{ns}
Ara-C	0.078 ± 0.019	–	0.111 ± 0.058	–	0.457 ± 0.155	–	2.961 ± 0.750	–
Ara-C + 3-BP $EC_{12.5}$	0.087 ± 0.007	0.9 ^{ns}	0.091 ± 0.053	1.2 ^{ns}	0.272 ± 0.091	1.6 ^{ns}	0.586 ± 0.158	5.1$^{\#\#}$
Ara-C + 3-BP EC_{25}	0.099 ± 0.039	0.8 ^{ns}	0.102 ± 0.063	1.1 ^{ns}	0.226 ± 0.105	2.0^{ns}	0.480 ± 0.051	6.2$^{\#\#\#}$

EC_{50} values were estimated by applying a sigmoidal dose-response non-linear regression. Results are the mean ± SD of triplicates of at least three independents experiments with at least two replicates each. One-way ANOVA followed by Dunnet's Multiple Comparison Test. ##p ≤ 0.01; ###p ≤ 0.001; ns, not significant.
[a] EC_{50} Chemotherapeutic drug/EC_{50} Chemotherapeutic drug + 3-BP.

Table 2
Effect of pre-treatment with 3-bromopyruvate (3-BP) on response to chemotherapy in AML cell lines.

	EC_{50} values ± SD (μM) for DNR and Ara-C in AML cells pre-treated or not with 3-BP							
Treatment	HL-60	Fold change[a] (EC_{50})	NB-4	Fold change (EC_{50})	KG-1	Fold change (EC_{50})	MOLM13	Fold change (EC_{50})
DNR	0.005 ± 0.003	–	0.015 ± 0.010	–	0.023 ± 0.004	–	0.013 ± 0.008	–
3-BP PT + DNR	0.004 ± 0.002	1.3 ^{ns}	0.011 ± 0.015	1.4 ^{ns}	0.005 ± 0.004	4.6$^{\#\#}$	0.017 ± 0.008	0.8^{ns}
Ara-C	0.072 ± 0.041	–	0.495 ± 0.531	–	0.644 ± 0.205	–	2.670 ± 1.138	–
3-BP PT + Ara-C	0.117 ± 0.069	0.6 ^{ns}	0.479 ± 0.265	1.0 ^{ns}	0.143 ± 0.022	4.5$^{\#}$	0.525 ± 0.316	5.1$^{\#}$

PT - 5 μM pre-treatment for 16 h.
EC_{50} values were estimated by applying a sigmoidal dose-response non-linear regression. Results are the mean ± SD of triplicates of at least three independents experiments with at least two replicates each. Statistical significance was estimated by the unpaired two-tailed Student's t-test: #$p \leq 0.05$; ##$p \leq 0.01$; ns, not significant.
[a] EC_{50} Chemotherapeutic drug/EC_{50} 3-BP PT → Chemotherapeutic drug.

[29–32]. However, KG-1 cells appear to exhibit metabolic flexibility [18], suggesting a balance between glycolysis and respiration, which could influence their response to chemotherapy and potential combinations with metabolic inhibitors.

In clinical practice, the combination of an anthracycline, (e.g. DNR) with an anti-metabolite, Ara-C [3,35], consists in the standard treatment of AML. The concentrations of Ara-C and DNR used in this study reflect clinically relevant ranges (~0.1–3.0 μM and 0.01–0.05 μM, respectively) observed in patients' plasma undergoing chemotherapy. Ara-C is typically administered at plasma concentrations of approximately 1–10 μM in standard-dose regimens, while high-dose therapy can result in concentrations of up to 100–200 μM [36,37]. For DNR, the peak plasma levels of range from approximately 1–2 μM [38–40]. Both drugs target DNA replication although with different mechanisms of action. A few different mechanisms have been described for DNR, such as intercalation with DNA, inhibition of topoisomerase II activity, and free-radical formation [41], while Ara-C is incorporated into DNA as a pyrimidine analog during the S phase of the cell cycle [42]. Although Ara-C is a mainstay of AML treatment, its cytotoxic mechanisms for inducing apoptosis are poorly understood. However, studies using AML cell lines

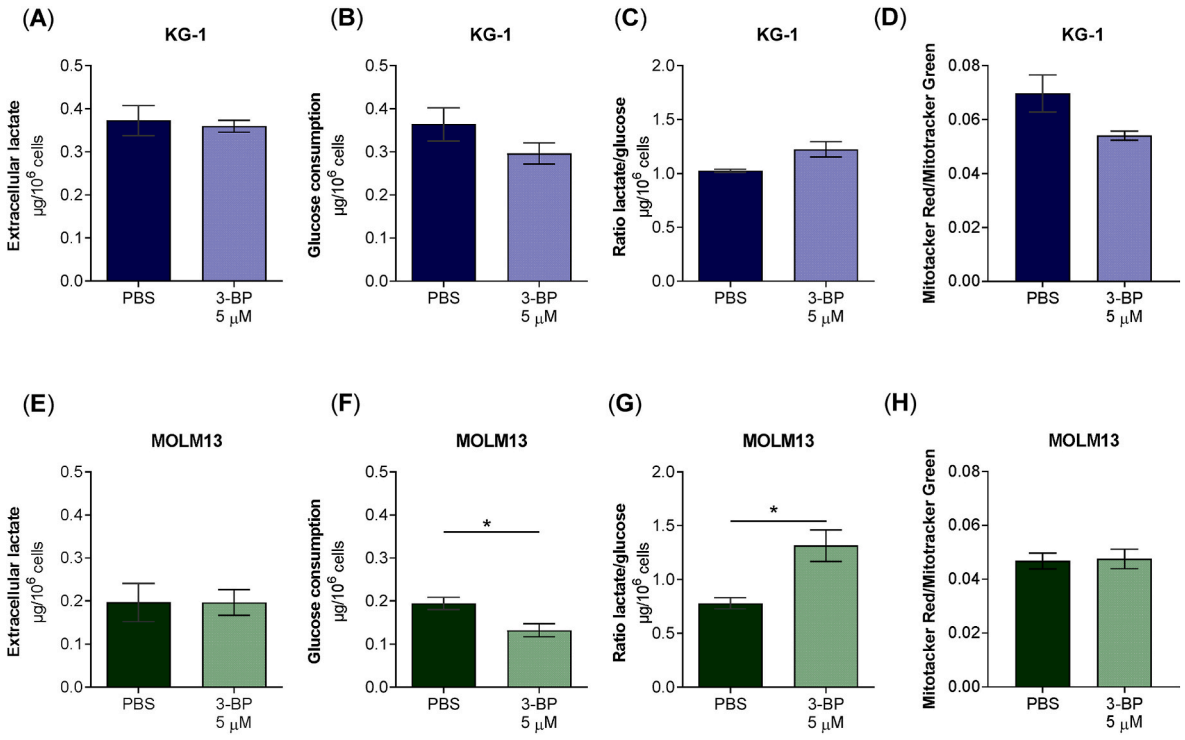

Fig. 4. Effect of the pre-treatment with 3-bromopyruvate (3-BP) on the glycolytic profile and mitochondrial activity of AML cell lines. (A–D) KG-1 and (E–H) MOLM13 cells were treated with 5 µM 3-BP for 16 h. Then, levels of extracellular lactate (A, E), glucose consumption (B, F), and ratio of lactate and glucose (C, G) were evaluated. (D, H) Mitochondrial activity was estimated by the mitochondrial polarization/mitochondrial mass ratio. MFI, mean fluorescence intensity. Results are from three independent experiments. Statistical significance was estimated by the unpaired two-tailed Student's t-test: $*p \leq 0.05$.

and human primary AML cells associated metabolic reprogramming with chemo-resistance, showing that enhanced glycolysis decreases AML cell sensitivity to Ara-C, while the inhibition of glycolysis improved drug cytotoxicity [11,14,15]. On the other hand, the ability of these anti-leukemic drugs to induce apoptosis through ROS production has been demonstrated, as well as the importance of the antioxidant capacity of AML cells to protect themselves from the drug effect [43,44].

Since metabolic reprogramming has been identified as a key factor influencing the effect of chemotherapy in AML, we aimed to explore the chemo-sensitizing properties of 3-BP. While its potential as an anti-cancer agent is well-documented, high doses have been associated with toxicity *in vivo* [16,45]. Chang et al. demonstrated that selective intra-arterial administration of 5–25 mM 3-BP in the rabbit model causes considerable toxic effects, not only in the liver but also in the gastrointestinal system. These effects (hemorrhagic pyloric, duodenal necrosis and hepatotoxicity) were dose-dependent, with high doses leading to death [45]. In this study, we aimed to use a low concentration of 3-BP to minimize its toxic effects. We showed that a non-toxic concentration of 5 µM did not affect cell viability.

In the present study, we demonstrated that the pre-treatment with a non-toxic concentration of 3-BP boosted the effect of the drugs, once again in the less glycolytic cell lines, KG-1 and MOLM13. 3-BP, a halogenated derivative of pyruvate, is mainly described as a glycolytic inhibitor [16,17], having two major anti-cancer mechanisms: it blocks energetic metabolism and induces cell death. As an MCT substrate, 3-BP selectively enters cancer cells via MCT1, and inhibits HKII activity by alkylation during glycolysis, suppressing the production of ATP [23]. HKII binds mitochondrial Voltage-Dependent Anion Channels (VDACs) that support the impermeabilization of mitochondrial membrane for activation of cell death pathways. Once 3-BP inhibits HKII, the cell death mediators can induce the release of cytochrome *c* located at the inter-membrane mitochondrial space [24]. Additionally, the effect of different concentrations of 3-BP were reported for HL-60 and NB-4. It was previously reported that 3-BP caused concentration-dependent cell death, metabolic inhibition, and glutathione (GSH) depletion of AML cells, inducing apoptosis and/or necrosis and oxidative stress at 20–30 µM [29]. Herein, we tested a lower concentration of 3-BP, 5 µM, where we did not observe an association between the effect of 3-BP with metabolism phenotype-associated protein expression neither with glycolytic profile nor with cell death induction. Considering the alkylating and oxidizing properties of 3-BP [16,17,29], we demonstrated that 5 µM 3-BP decreased the AML antioxidant capacity, depleting the reduced GSH levels by ROS production. GSH can act directly as an antioxidant to protect cells against free radicals and pro-oxidants, as well as a cofactor for antioxidant and detoxification enzymes such as glutathione peroxidases and glutathione S-transferases [46]. Other studies have also provided evidence that 3-BP may attack cysteine residues present in GSH, as a thiol blocker [47,48].

The results show a difference in basal GSH levels between KG-1 and MOLM13 cells, which suggests that KG-1 cells may be more resistant to oxidative stress-inducing treatments, such as 3-BP. This aligns with our observations, where NAC, a GSH precursor, provides a protective effect (Fig. 6), likely through a ROS scavenging effect [47]. Although KG-1 cells could have greater antioxidant defenses compared to MOLM13, 3-BP may overcome these defenses, by exacerbating DNR-induced oxidative stress and leading to increased cytotoxicity [49]. In contrast, MOLM13 cells, which have lower basal ROS levels and a preference for OXPHOS metabolism [18,34], may be less susceptible to oxidative stress-inducing agents. On the other hand, both cell lines were more sensitive to Ara-C after 3-BP pre-treatment. Despite its main mechanism of action of incorporation of the drug into DNA, there is evidence that Ara-C induces oxidative stress in leukemic cells by generating ROS [50].

The role of ROS in cancer, including in AML is paradoxical. Depending on the context, ROS, and antioxidants can either promote or prevent tumor formation or progression [43,49]. High ROS levels can induce nuclear factor erythroid 2-related factor 2 (Nrf2) nuclear translocation in cells, leading to metabolic reprogramming [51]. At the same time, Nrf2 is a major regulator of oxidative stress resistance. Upon

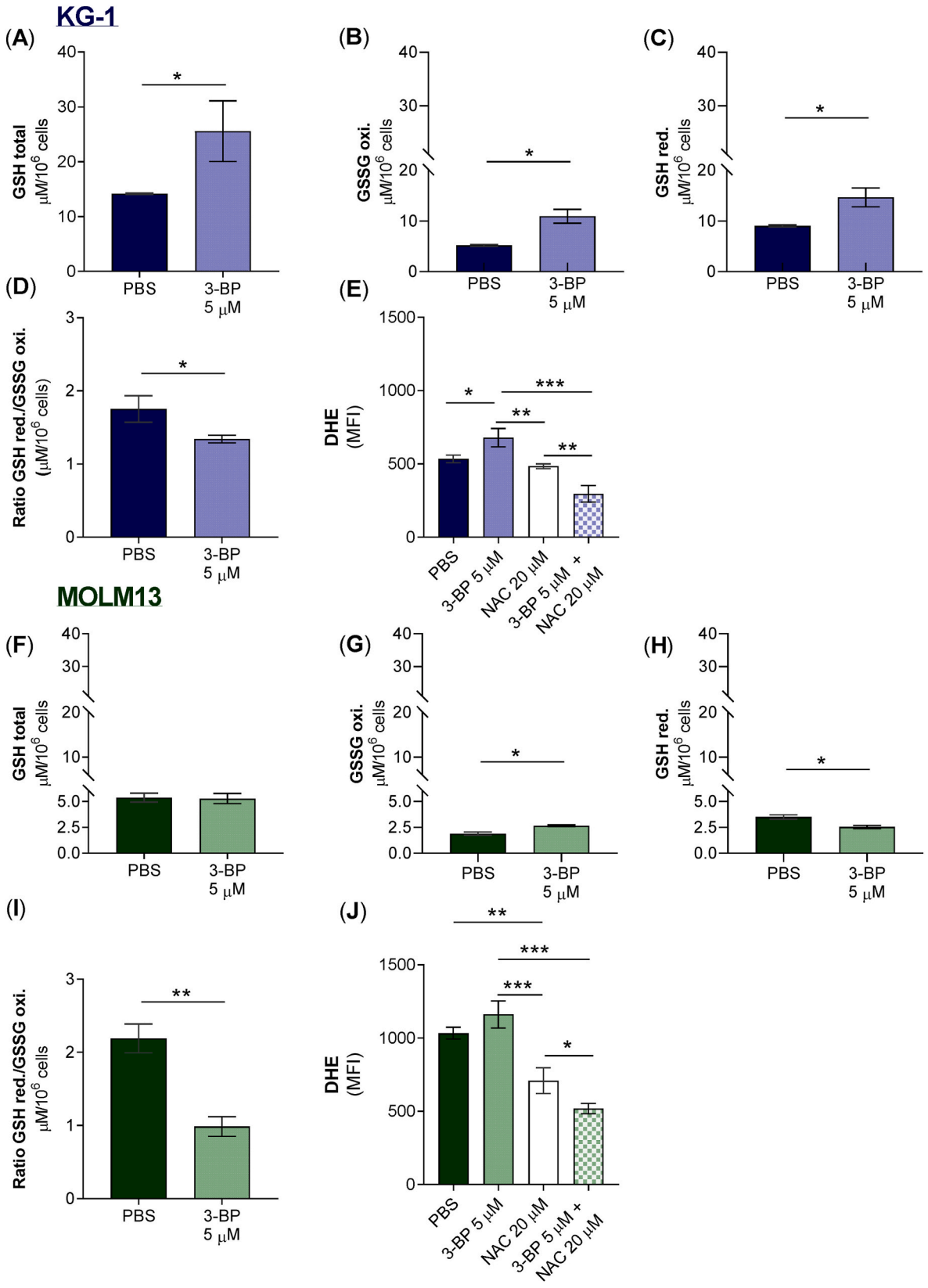

Fig. 5. Effect of the pre-treatment with 3-bromopyruvate (3-BP) on the antioxidant capacity of AML cell lines. (A, F) Total, (B, G) oxidized and (C, H) reduced glutathione (GSH, GSSG oxi., GSH red., respectively) levels were assessed after treatment with 5 µM 3-BP for 16 h (colorimetric kit) and (D, I) the ratio of GSH red./GSSG oxi calculated in (A–E) KG-1 and (F–J) MOLM13 cell lines. Data were normalized to the number of cells. Statistical significance was estimated by the unpaired two-tailed Student's t-test. (E, J) Production of reactive oxygen species (ROS) was measured using flow cytometry. MFI, mean fluorescence intensity; N-acetyl cysteine (NAC). Statistical significance was estimated by the unpaired two-tailed Student's t-test (A-D, F-I) and one-way ANOVA followed by Tukey's Multiple Comparison Test (E, H): *p ≤ 0.05; **p ≤ 0.01; ***p ≤ 0.001. (For interpretation of the references to color in this figure legend, the reader is referred to the Web version of this article.)

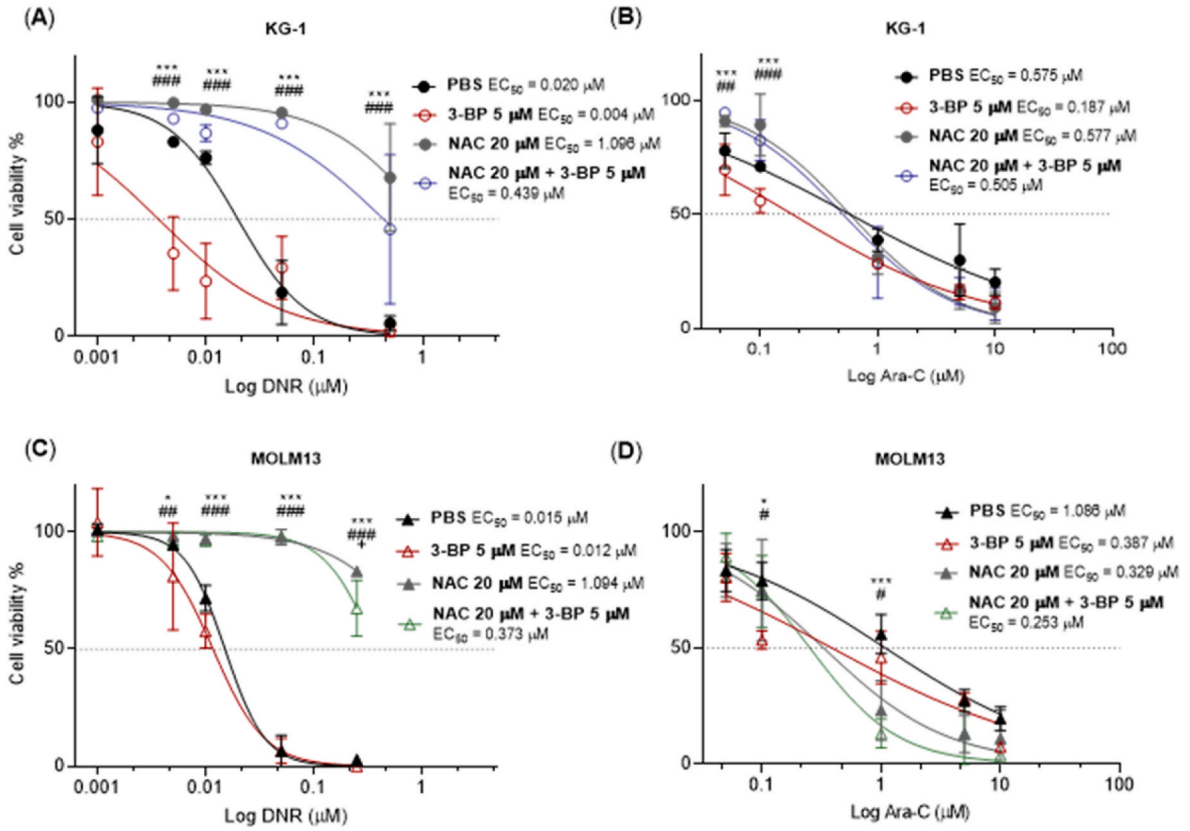

Fig. 6. Effect of N-acetylcysteine (NAC) on the effect of 3-bromopyruvate (3-BP) in the response of AML cells to chemotherapy. Dose-response curve to generate IC_{50} values of KG-1 (A, B) and MOLM13 (C, D) cell lines in response to DNR (A, C) and Ara-C (B, D). Values are expressed as cell viability relative to vehicle-treated (PBS) cells normalized to 100 %. Values are given as mean ± SD. Results are from three independent experiments with two replicates each. Two-way ANOVA followed by Dunnet's Multiple Comparison Test. *, #, + $p \leq 0.05$; ##$p \leq 0.01$; ***, ###$p \leq 0.001$; ns, not significant. Comparing groups: 3-BP 5 μM vs NAC 20 μM + 3-BP 5 μM (*), NAC 20 μM vs 3-BP 5 μM (#), or NAC 20 μM vs NAC 20 μM + 3-BP 5 μM (+).

activation, Nrf2 translocates to the nucleus and binds antioxidant response elements, triggering the expression of antioxidant genes [49,52] Interestingly, there is evidence that NAC, which typically reduces oxidative stress, can also increase Nrf2 expression [53,54]. This could explain why NAC, a ROS scavenger, not only protects cells from the effects of 3-BP and chemotherapy but may also enhance their effects in MOLM13 cells.

The mechanism of action of classical drugs used long ago in the treatment of hematological malignancies, favors pro-oxidant mechanisms [43]. Apart from increasing ROS, this approach can lead to damage of lipids and proteins, DNA mutations, mitochondrial stress, reduced antioxidant capacity, and cell cycle arrest, all of which have been implicated in cell injury and cell death [29–33,35,41,42,44]. However, prolonged exposure to chemotherapy-induced ROS may increase genetic instability in cancer cells due to ROS-induced mutations and in this way contributes to the high toxicity of treatment and eventually, chemoresistance in AML patients [55–57]. In our study, we envisaged a strategy to boost the chemotherapy effect by combining 3-BP with conventional chemotherapeutic drugs and simultaneously decreasing their toxicity. The effect of 3-BP as a chemo-sensitizing agent was tested by two approaches: i) a combination of low concentrations of 3-BP simultaneously with the DNR and Ara-C and ii) a pre-treatment with a non-toxic concentration followed by the drugs. It became evident that both strategies boosted the effect of chemotherapy only in the MOLM13 and KG-1 cell lines, with pre-treatment having a greater effect by decreasing cell viability and consequently a significant decrease of EC_{50} values for DNR and Ara-C.

Overall, in the different AML cell line models used in this study, we were able to highlight the importance of incorporating a metabolic characterization and antioxidant capacity of the malignant cells to guide the selection of therapeutic strategies in such a heterogeneous disease. We demonstrated the chemo-sensitizing activity of 3-BP was mainly due to its capacity to weaken AML antioxidant capacity.

5. Conclusions

Herein, we used four AML cell lines that had different metabolic profiles and different responses to 3-BP. Combination with 3-BP boosted the effect of chemotherapy in the less glycolytic cells, MOLM13 and KG-1, with the pre-treatment strategy having the greatest effect by decreasing DNR and Ara-C EC_{50} values. The increase in ROS levels induced by 3-BP pre-treatment appears to be responsible for boosting the effect of DNR and Ara-C, by decreasing their effective concentrations. Further, treating cells with the ROS scavenger NAC, not only protects cells from the effect of 3-BP and chemotherapy but may also have chemotherapy effect, depending on the cell type and drug. Thus, combination of chemotherapy with ROS-inducing drugs has the potential to boost the response of AML cells to chemotherapy, which should be further explored in clinics, not only to enhance the effectiveness of treatment but also to decrease its associated toxicity.

CRediT authorship contribution statement

Joana Pereira-Vieira: Writing – review & editing, Writing – original draft, Methodology, Investigation, Formal analysis, Conceptualization. **Sara Granja:** Writing – review & editing, Methodology, Investigation. **Sónia Pires Celeiro:** Writing – review & editing, Methodology, Investigation. **Catarina Barbosa-Matos:** Writing – review & editing,

Methodology, Investigation, Formal analysis. **Ana Preto:** Writing – review & editing, Conceptualization. **Odília Queirós:** Writing – review & editing, Conceptualization. **Young Hee Ko:** Writing – review & editing, Funding acquisition, Conceptualization. **Margarida Casal:** Writing – review & editing, Supervision, Funding acquisition, Conceptualization. **Fátima Baltazar:** Writing – review & editing, Supervision, Resources, Project administration, Funding acquisition, Conceptualization.

Funding

The work presented was conducted at the Life and Health Sciences Research Institute (ICVS), University of Minho. Financial support was provided by the Foundation for Science and Technology (FCT) through the Scientific Microscopy Platform of ICVS, as part of the national infrastructure Portuguese Platform of Bioimaging (PPBI, ref. PPBI-POCI-01-0145-FEDER-022122). FCT also supported four fellowship grants awarded to J.P-V., S.P.C., and C.B-M. (ref. SFRH/BD/146065/2019, 2020.05779.BD, SFRH/BD/145955/2019, and COVID/BD/153456/2023). Additional funding was granted through the Norte Portugal Regional Operational Program and the European Regional Development Fund (ERDF) and Norte Portugal Regional Operational Program (NORTE 2020) under the following references: UIDB/50026/2020, UIDP/50026/2020, NORTE-01-0145-FEDER-000039, NORTE-01-0145-FEDER-000055, and UID/BIA/04050/2020 (https://doi.org/10.54499/UIDB/04050/2020). Additional financial support was provided by NewG Lab Pharma.

Declaration of competing interest

The authors declare the following financial interests/personal relationships which may be considered as potential competing interests: Fatima Baltazar reports financial support was provided by NewG Lab Pharma. Young Hee Ko reports a relationship with NewG Lab Pharma that includes: board membership. The co-author Young Hee Ko was co-founder of NewG Lab Pharma. If there are other authors, they declare that they have no known competing financial interests or personal relationships that could have appeared to influence the work reported in this paper.

Acknowledgments

We thank Prof. Paula Ludovico (Life and Health Sciences Research Institute (ICVS)/School of Medicine/University of Minho, Braga, Portugal) for sharing the HL-60, NB-4, and KG-1 cell lines.

Appendix A. Supplementary data

Supplementary data to this article can be found online at https://doi.org/10.1016/j.freeradbiomed.2025.04.017.

References

[1] D.A. Arber, et al., The 2016 revision to the World Health Organization classification of myeloid neoplasms and acute leukemia, Blood 127 (20) (May 2016) 2391–2405, https://doi.org/10.1182/blood-2016-03-643544.
[2] A.K. Burnett, Treatment of acute myeloid leukemia: are we making progress? Hematology Am Soc Hematol Educ Program 2012 (2012) 1–6, https://doi.org/10.1182/asheducation-2012.1.1.
[3] H. Döhner, et al., Diagnosis and management of AML in adults: 2022 recommendations from an international expert panel on behalf of the ELN, Blood 140 (12) (Sep. 2022) 1345–1377, https://doi.org/10.1182/blood.2022016867.
[4] H.A. Abbas, M. Alfayez, T. Kadia, F. Ravandi-Kashani, N. Daver, Midostaurin in acute myeloid leukemia: an evidence-based review and patient selection, Cancer Manag. Res. 11 (2019) 8817–8828, https://doi.org/10.2147/CMAR.S177894.
[5] B.J. Wouters, Targeting IDH1 and IDH2 mutations in acute myeloid leukemia: emerging options and pending questions, HemaSphere 5 (6) (Jun. 2021) e583, https://doi.org/10.1097/HS9.0000000000000583.
[6] Y. Wei, et al., Targeting bcl-2 proteins in acute myeloid leukemia, Front. Oncol. 10 (Nov. 2020) 584974, https://doi.org/10.3389/fonc.2020.584974.
[7] C. Liu, Y. Jin, Z. Fan, The mechanism of warburg effect-induced chemoresistance in cancer, Front. Oncol. 11 (2021) 698023, https://doi.org/10.3389/fonc.2021.698023.
[8] O. Warburg, On the origin of cancer cells, Science 123 (3191) (Feb. 1956) 309–314, https://doi.org/10.1126/science.123.3191.309.
[9] D. Hanahan, Hallmarks of cancer: new dimensions, Cancer Discov. 12 (1) (Jan. 2022) 31–46, https://doi.org/10.1158/2159-8290.CD-21-1059.
[10] R.J. DeBerardinis, N.S. Chandel, Fundamentals of cancer metabolism, Sci. Adv. 2 (5) (May 2016) e1600200, https://doi.org/10.1126/sciadv.1600200.
[11] W.-L. Chen, et al., A distinct glucose metabolism signature of acute myeloid leukemia with prognostic value, Blood 124 (10) (Sep. 2014) 1645–1654, https://doi.org/10.1182/blood-2014-02-554204.
[12] K. Song, M. Li, X. Xu, L. Xuan, G. Huang, Q. Liu, Resistance to chemotherapy is associated with altered glucose metabolism in acute myeloid leukemia, Oncol. Lett. 12 (1) (Jul. 2016) 334–342, https://doi.org/10.3892/ol.2016.4600.
[13] L. Poulain, et al., High mTORC1 activity drives glycolysis addiction and sensitivity to G6PD inhibition in acute myeloid leukemia cells, Leukemia 31 (11) (Nov. 2017) 11, https://doi.org/10.1038/leu.2017.81.
[14] P.M. Herst, R.A. Howman, P.J. Neeson, M.V. Berridge, D.S. Ritchie, The level of glycolytic metabolism in acute myeloid leukemia blasts at diagnosis is prognostic for clinical outcome, J. Leukoc. Biol. 89 (1) (Jan. 2011) 51–55, https://doi.org/10.1189/jlb.0710417.
[15] P.M. Herst, E.L. Hesketh, D.S. Ritchie, M.V. Berridge, Glycolytic metabolism confers resistance to combined all-trans retinoic acid and arsenic trioxide-induced apoptosis in HL60ρ0 cells, Leuk. Res. 32 (2) (Feb. 2008) 327–333, https://doi.org/10.1016/j.leukres.2007.04.014.
[16] J. Azevedo-Silva, et al., The anticancer agent 3-bromopyruvate: a simple but powerful molecule taken from the lab to the bedside, J. Bioenerg. Biomembr. 48 (4) (Aug. 2016) 349–362, https://doi.org/10.1007/s10863-016-9670-z.
[17] Y.H. Ko, P.L. Pedersen, J.F. Geschwind, Glucose catabolism in the rabbit VX2 tumor model for liver cancer: characterization and targeting hexokinase, Cancer Lett. 173 (1) (Nov. 2001) 83–91, https://doi.org/10.1016/s0304-3835(01)00667-x.
[18] J. Pereira-Vieira, et al., Glucose metabolism as a potential therapeutic target in cytarabine-resistant acute myeloid leukemia, Pharmaceutics 16 (4) (Mar. 2024) 442, https://doi.org/10.3390/pharmaceutics16040442.
[19] E. Saulle, et al., Targeting lactate metabolism by inhibiting MCT1 or MCT4 impairs leukemic cell proliferation, induces two different related death-pathways and increases chemotherapeutic sensitivity of acute myeloid leukemia cells, Front. Oncol. 10 (2020) 621458, https://doi.org/10.3389/fonc.2020.621458.
[20] C. Pinheiro, A. Longatto-Filho, J. Azevedo-Silva, M. Casal, F.C. Schmitt, F. Baltazar, Role of monocarboxylate transporters in human cancers: state of the art, J. Bioenerg. Biomembr. 44 (1) (Feb. 2012) 127–139, https://doi.org/10.1007/s10863-012-9428-1.
[21] F. Lopes-Coelho, et al., Monocarboxylate transporter 1 (MCT1), a tool to stratify acute myeloid leukemia (AML) patients and a vehicle to kill cancer cells, Oncotarget 8 (47) (Aug. 2017) 82803–82823, https://doi.org/10.18632/oncotarget.20294.
[22] F. Baltazar, et al., Monocarboxylate transporters as targets and mediators in cancer therapy response, Histol. Histopathol. 29 (12) (Dec. 2014) 1511–1524, https://doi.org/10.14670/HH-29.1511.
[23] T. Fan, G. Sun, X. Sun, L. Zhao, R. Zhong, Y. Peng, Tumor energy metabolism and potential of 3-bromopyruvate as an inhibitor of aerobic glycolysis: implications in tumor treatment, Cancers (Basel) 11 (3) (Mar. 2019) 317, https://doi.org/10.3390/cancers11030317.
[24] T.-A. Wang, X.-D. Zhang, X.-Y. Guo, S.-L. Xian, Y.-F. Lu, 3-bromopyruvate and sodium citrate target glycolysis, suppress survivin, and induce mitochondrial-mediated apoptosis in gastric cancer cells and inhibit gastric orthotopic transplantation tumor growth, Oncol. Rep. 35 (3) (Mar. 2016) 1287–1296, https://doi.org/10.3892/or.2015.4511.
[25] A. Pereira-Nunes et al., "Combination Therapy With CD147-Targeted Nanoparticles Carrying Phenformin Decreases Lung Cancer Growth - Pereira-Nunes - 2023 - Advanced Biology - Wiley Online Library," Combination Therapy With CD147-Targeted Nanoparticles Carrying Phenformin Decreases Lung Cancer Growth. Accessed: December. 2, 2023. [Online]. Available: https://onlinelibrary.wiley.com/doi/10.1002/adbi.202300080.
[26] V. Miranda-Gonçalves, et al., MCT1 is a new prognostic biomarker and its therapeutic inhibition boosts response to temozolomide in human glioblastoma, Cancers (Basel) 13 (14) (Jul. 2021) 3468, https://doi.org/10.3390/cancers13143468.
[27] D. Tavares-Valente, S. Granja, F. Baltazar, O. Queirós, Bioenergetic modulators hamper cancer cell viability and enhance response to chemotherapy, J. Cell Mol. Med. 22 (8) (Aug. 2018) 3782–3794, https://doi.org/10.1111/jcmm.13642.
[28] R. Amorim, et al., Monocarboxylate transport inhibition potentiates the cytotoxic effect of 5-fluorouracil in colorectal cancer cells, Cancer Lett. 365 (1) (Aug. 2015) 68–78, https://doi.org/10.1016/j.canlet.2015.05.015.
[29] E. Calviño, et al., Regulation of death induction and chemosensitizing action of 3-bromopyruvate in myeloid leukemia cells: energy depletion, oxidative stress, and protein kinase activity modulation, J. Pharmacol. Exp. Therapeut. 348 (2) (Feb. 2014) 324–335, https://doi.org/10.1124/jpet.113.206714.
[30] X. Yu, et al., Inhibition of NRF2 enhances the acute myeloid leukemia cell death induced by venetoclax via the ferroptosis pathway, Cell Death Discov. 10 (1) (Jan. 2024) 1–10, https://doi.org/10.1038/s41420-024-01800-2.
[31] O. Pereira, A. Teixeira, B. Sampaio-Marques, I. Castro, H. Girão, P. Ludovico, Signalling mechanisms that regulate metabolic profile and autophagy of acute

myeloid leukaemia cells, J. Cell Mol. Med. 22 (10) (Oct. 2018) 4807–4817, https://doi.org/10.1111/jcmm.13737.
[32] B. Yucel, M. Sonmez, Repression of oxidative phosphorylation sensitizes leukemia cell lines to cytarabine, Hematology 23 (6) (Jul. 2018) 330–336, https://doi.org/10.1080/10245332.2017.1402454.
[33] Leibniz Institute DSMZ: Details." Accessed: Jun. 11, 2024. [Online]. Available: https://www.dsmz.de/collection/catalogue/details/culture/ACC-3.
[34] A. Erdem, et al., The Glycolytic Gatekeeper PDK1 defines different metabolic states between genetically distinct subtypes of human acute myeloid leukemia, Nat. Commun. 13 (1) (Mar. 2022) 1105, https://doi.org/10.1038/s41467-022-28737-3.
[35] M.A. Lichtman, A historical perspective on the development of the cytarabine (7days) and daunorubicin (3days) treatment regimen for acute myelogenous leukemia: 2013 the 40th anniversary of 7+3, Blood Cells Mol. Dis. 50 (2) (Feb. 2013) 119–130, https://doi.org/10.1016/j.bcmd.2012.10.005.
[36] A. Hamada, T. Kawaguchi, M. Nakano, Clinical pharmacokinetics of cytarabine formulations, Clin. Pharmacokinet. 41 (10) (2002) 705–718, https://doi.org/10.2165/00003088-200241100-00002.
[37] M. Takeuchi, T. Yamauchi, I. Yoshida, R. Soda, T. Ueda, K. Takahashi, Pharmacokinetics of a standard dose of cytarabine in a patient with acute promyelocytic leukemia undergoing continuous ambulatory peritoneal dialysis, Int. J. Hematol. 77 (2) (Feb. 2003) 196–198, https://doi.org/10.1007/BF02983222.
[38] P.H. Houba, et al., Distribution and pharmacokinetics of the prodrug daunorubicin-GA3 in nude mice bearing human ovarian cancer xenografts, Biochem. Pharmacol. 57 (6) (Mar. 1999) 673–680, https://doi.org/10.1016/s0006-2952(98)00343-8.
[39] R. Di Francia, et al., Response and toxicity to cytarabine therapy in leukemia and lymphoma: from dose puzzle to pharmacogenomic biomarkers, Cancers (Basel) 13 (5) (Feb. 2021) 966, https://doi.org/10.3390/cancers13050966.
[40] T.L. Lin, et al., A phase 2 study to assess the pharmacokinetics and pharmacodynamics of CPX-351 and its effects on cardiac repolarization in patients with acute leukemias, Cancer Chemother. Pharmacol. 84 (1) (Jul. 2019) 163–173, https://doi.org/10.1007/s00280-019-03856-9.
[41] D.A. Gewirtz, A critical evaluation of the mechanisms of action proposed for the antitumor effects of the anthracycline antibiotics adriamycin and daunorubicin, Biochem. Pharmacol. 57 (7) (Apr. 1999) 727–741, https://doi.org/10.1016/s0006-2952(98)00307-4.
[42] R.L. Momparler, Optimization of cytarabine (ARA-C) therapy for acute myeloid leukemia, Exp. Hematol. Oncol. 2 (2013) 20, https://doi.org/10.1186/2162-3619-2-20.
[43] N.M. Kaweme, S. Zhou, G.J. Changwe, F. Zhou, The significant role of redox system in myeloid leukemia: from pathogenesis to therapeutic applications, Biomark. Res. 8 (1) (Nov. 2020) 63, https://doi.org/10.1186/s40364-020-00242-z.
[44] S.-A. Heasman, L. Zaitseva, K.M. Bowles, S.A. Rushworth, D.J. Macewan, Protection of acute myeloid leukaemia cells from apoptosis induced by front-line chemotherapeutics is mediated by haem oxygenase-1, Oncotarget 2 (9) (Sep. 2011) 658–668, https://doi.org/10.18632/oncotarget.321.
[45] J.M. Chang, et al., Local toxicity of hepatic arterial infusion of hexokinase II inhibitor, 3-bromopyruvate: in vivo investigation in normal rabbit model, Acad. Radiol. 14 (1) (Jan. 2007) 85–92, https://doi.org/10.1016/j.acra.2006.09.059.
[46] D.A. Averill-Bates, Chapter Five - the antioxidant glutathione, in: G. Litwack (Ed.), Vitamins and Hormones, Antioxidants, vol. 121, Academic Press, 2023, pp. 109–141, https://doi.org/10.1016/bs.vh.2022.09.002, 121.
[47] S.M. El Sayed, H. Baghdadi, M. Zolaly, H.H. Almaramhy, M. Ayat, J.G. Donki, The promising anticancer drug 3-bromopyruvate is metabolized through glutathione conjugation which affects chemoresistance and clinical practice: an evidence-based view, Med. Hypotheses 100 (Mar. 2017) 67–77, https://doi.org/10.1016/j.mehy.2017.01.014.
[48] K. Niedźwiecka, et al., Glutathione may have implications in the design of 3-bromopyruvate treatment protocols for both fungal and algal infections as well as multiple myeloma, Oncotarget 7 (40) (Oct. 2016) 65614–65626, https://doi.org/10.18632/oncotarget.11592.
[49] C. Fan, X. Yang, L. Yan, Z. Shi, Oxidative stress is two-sided in the treatment of acute myeloid leukemia, Cancer Med. 13 (9) (2024) e6806, https://doi.org/10.1002/cam4.6806.
[50] M. Sadeghi, et al., The sensitivity of acute myeloid leukemia cells to cytarabine is increased by suppressing the expression of Heme oxygenase-1 and hypoxia-inducible factor 1-alpha, Cancer Cell Int. 24 (1) (Jun. 2024) 217, https://doi.org/10.1186/s12935-024-03393-3.
[51] R. Wang, L. Liang, M. Matsumoto, K. Iwata, A. Umemura, F. He, Reactive oxygen species and NRF2 signaling, friends or foes in cancer? Biomolecules 13 (2) (Feb. 2023) 353, https://doi.org/10.3390/biom13020353.
[52] S. Vomund, A. Schäfer, M.J. Parnham, B. Brüne, A. Von Knethen, Nrf2, the master regulator of anti-oxidative responses, Int. J. Mol. Sci. 18 (12) (Dec. 2017) 12, https://doi.org/10.3390/ijms18122772.
[53] R. Jannatifar, K. Parivar, N. Hayati Roodbari, M.H. Nasr-Esfahani, The effect of N-Acetyl-Cysteine on NRF2 antioxidant gene expression in asthenoteratozoospermia men: a clinical trial study, Int J Fertil Steril 14 (3) (2020) 171–175, https://doi.org/10.22074/ijfs.2020.44411.
[54] B. Kalyanaraman, NAC, NAC, Knockin' on Heaven's door: interpreting the mechanism of action of *N*-acetylcysteine in tumor and immune cells, Redox Biol. 57 (Nov. 2022) 102497, https://doi.org/10.1016/j.redox.2022.102497.
[55] A. Sallmyr, et al., Internal tandem duplication of FLT3 (FLT3/ITD) induces increased ROS production, DNA damage, and misrepair: implications for poor prognosis in AML, Blood 111 (6) (Mar. 2008) 3173–3182, https://doi.org/10.1182/blood-2007-05-092510.
[56] E.D. Lagadinou, et al., BCL-2 inhibition targets oxidative phosphorylation and selectively eradicates quiescent human leukemia stem cells, Cell Stem Cell 12 (3) (Mar. 2013) 329–341, https://doi.org/10.1016/j.stem.2012.12.013.
[57] J.R. Sillar, Z.P. Germon, G.N. De Iuliis, M.D. Dun, The role of reactive oxygen species in acute myeloid leukaemia, Int. J. Mol. Sci. 20 (23) (Nov. 2019) 6003, https://doi.org/10.3390/ijms20236003.